$LaTeBO_5$: a new borotellurite with a large birefringence activated by the highly distorted $[Te^{(iv)}O_4]$ group

Jiankang Wang,[a] Hongping Wu,[a] Hongwei Yu,[a,*] Zhanggui Hu,[a] Jiyang Wang,[a] Yicheng Wu[a]

[a]Tianjin Key Laboratory of Functional Crystal Materials, Institute of Functional Crystal, Materials Science and Engineering, Tianjin University of Technology, Tianjin 300384, China.
E-mail: hwyu15@gmail.com

CONTENTS

Experimental section

Synthesis of polycrystalline $LaTeBO_5$.

The polycrystalline samples of $LaTeBO_5$ were synthesized by the traditional solid-state reactions technology. The stoichiometric ratio (1:1:1) of La_2O_3 (99.99%, Aladdin Chemistry Co., Ltd.), TeO_2 (99.99%, Aladdin Chemistry Co., Ltd.) and H_3BO_3 (99.99%, Aladdin Chemistry Co., Ltd.) were thoroughly ground and then packed into a crucible and preheated from 25 to 300 ℃ at a rate of 4 ℃/min in a furnace. In order to obtain pure phase $LaTeBO_5$, the temperature was raised to 710 ℃ at a rate of 4 ℃/min and kept at this temperature for 70 h with several intermediate grinding. The experimental XRD powder spectrum of $LaTeBO_5$ is according with the calculated one from its single-crystal XRD data.

Single crystal synthesis.

The single crystal of $LaTeBO_5$ was obtained through the high temperature melting method. In order to reduce the viscosity of La-Te-B-O system, PbO was used as a flux. The mixtures of La_2O_3, TeO_2, H_3BO_3 and PbO with a molar ratio of 1:2:1:2 were slowly heated up to 680 ℃ at a rate 4 ℃/min and maintained at this temperature for 8 h to obtain a transparent and homogeneous melt. Then the melt was lowered to crystallization temperature 630 ℃ at a rate 3 ℃/h and followed by a cooling rate of 20 ℃/h to 30 ℃. Finally, a colorless and transparent single crystal was obtained.

Powder X-ray diffraction.

The single phase of $LaTeBO_5$ powder data was collected from 10° to 70° (2θ) with a step width size of 0.01° and a step time of 2 s used a SmartLab9KW powder X-ray diffractometer with Cu-Kα radiation.

Structure determination.

The crystal structure of $LaTeBO_5$ was detected by single-crystal X-ray diffraction equipment with a Bruker SMART APEX Ⅲ CCD diffractometer and Mo Kα radiation (λ = 0.71073 Å) at 293(2) K. The data integration, cell refine and absorption were carried out by the SAINT program.[1] The crystal structure was solved used the SHELXTL crystallographic software package.[2] The crystal data and structure refinement parameters are shown in Table S1. Some structural parameters including final refined atomic positions, isotropic thermal parameters and main interatomic distances and angles are exhibited in Table S2 and Table S3, respectively.

Energy-Dispersive X-Ray spectroscope (EDX).

Microprobe elemental analyses and the elemental distribution maps were performed using an energy dispersive X-ray spectroscope with a field-emission scanning electron microscope (FESEM, Quanta FEG 250) made by FEI.

UV−Vis−NIR diffuse reflectance spectrum.

The Shimadzu SolidSpec-3700DUV spectrophotometer was employed to measure UV−Vis−NIR diffuse reflectance spectrum of $LaTeBO_5$ in a wavelength range from 190 to 2600 nm at room temperature. According to the Kubelka–Munk function[3]: $F(R) = (1- R)^2/2R = K/S$ (R = reflectance; K = absorption; S = scattering), the reflectance spectrum was converted to absorption spectrum.

Infrared spectroscopy.

The Nicolet iS50 FT-IR spectrometer was employed to record the infrared spectrum of $LaTeBO_5$ in the range 400-4000 cm^{-1}.

Thermal stability.

The thermal characteristic of $LaTeBO_5$ was evaluated on differential scanning calorimetry (DSC) and thermogravimetric analysis (TG) using a STA449 F5 DSC/TG analyzer (NETZSCH Instruments). In nitrogen atmosphere, the purity phase of $LaTeBO_5$ was packed into platinum crucible and raised to 1300℃ at a rate of 5℃/min and followed by cooling to room temperature under the same rate.

Theoretical calculation.

The band structures, the total and partial density of states and the optical properties of $LaTeBO_5$ were calculated by a plane-wave pseudopotential density functional theory (DFT) method employed on CASTEP program.[4] The generalized gradient approximation (GGA)[5] with the Perdew–Burke–Ernzerhof function[6] was setting as exchange–correlation function. The valence states were treated as follows: La-$5d^1 6s^2$, Te-$5s^2 5p^4$, B-$2s^2 2p^1$, O-$2s^2 2p^4$ under the norm-conserving pseudopotential. The energy cutoff of the plane wave was set as 830 eV and the k-point grid sampling in the Monkhorst Pack scheme was set at 2 × 4 × 2 in the Brillouin zone.[7]

Table S1. Crystal data and structure refinement for $LaTeBO_5$.

Empirical formula	$LaTeBO_5$
Formula weight	357.32
Temperature	293(2) K
Wavelength	0.71073 Å
Crystal system	Orthorhombic
Space group	*Pbca*
Unit cell dimensions	a = 10.8220(5) Å
	b = 6.9216(3) Å
	c = 11.5812(5) Å
Z	8
Absorption coefficient	16.350 mm^{-1}
F(000)	1232
Reflections collected	5367
Independent reflections	997 [R_{int} = 0.1015]
Completeness to theta = 25.242°	100.0 %
Data / restraints / parameters	997 / 0 / 73
Goodness-of-fit on F^2	0.972
Final R indices [I>2sigma(I)] [a]	R_1 = 0.0279, wR_2 = 0.0733
R indices (all data) [a]	R_1 = 0.0310, wR_2 = 0.0770
Largest diff. peak and hole	1.611 and -1.996 e·$Å^{-3}$

[a] $R_1 = \Sigma||F_o| - |F_c||/\Sigma|F_o|$ and $wR^2 = [\Sigma w(F_o^2 - F_c^2)^2 / \Sigma w F_o^4]^{1/2}$ for $F_o^2 > 2\sigma(F_o^2)$

Table S2. Atomic coordinates ($\times 10^4$) and equivalent isotropic displacement parameters ($Å^2 \times 10^3$) for $LaTeBO_5$. U_{eq} is defined as one third of the trace of the orthogonalized U_{ij} tensor.

Atoms	x	y	z	U_{eq}	BVS
La(1)	5105(1)	5320(1)	6766(1)	6(1)	3.16
B(1)	7539(6)	2399(10)	7319(5)	7(1)	2.98
Te(1)	6411(1)	855(1)	4983(1)	7(1)	3.92
O(1)	7686(4)	1407(6)	6252(3)	11(1)	2.02
O(2)	5835(4)	3388(6)	5061(3)	11(1)	2.15
O(3)	5302(4)	-277(7)	6049(4)	10(1)	2.05
O(4)	6387(4)	2830(6)	7685(3)	8(1)	2.09
O(5)	8586(4)	2676(6)	7932(4)	10(1)	1.91

Table S3. Selected bond distances (Å) and angles (deg).

La(1)-O(4)#1	2.455(4)	O(2)#3-La(1)-O(3)#1	143.81(14)
La(1)-O(4)	2.455(4)	O(2)-La(1)-O(3)#1	137.15(14)
La(1)-O(5)#2	2.485(4)	O(5)#4-La(1)-O(3)#1	71.36(14)
La(1)-O(2)#3	2.512(4)	O(1)#4-La(1)-O(3)#1	115.37(13)
La(1)-O(2)	2.513(4)	O(4)#1-La(1)-B(1)#4	99.46(16)
La(1)-O(5)#4	2.548(4)	O(4)-La(1)-B(1)#4	76.33(16)
La(1)-O(1)#4	2.576(4)	O(5)#2-La(1)-B(1)#4	152.42(16)
La(1)-O(3)#1	2.601(4)	O(2)#3-La(1)-B(1)#4	110.72(16)
La(1)-B(1)#4	2.997(7)	O(2)-La(1)-B(1)#4	98.96(17)
La(1)-Te(1)#3	3.7151(5)	O(5)#4-La(1)-B(1)#4	26.64(15)
La(1)-La(1)#5	3.8624(3)	O(1)#4-La(1)-B(1)#4	28.32(15)
La(1)-La(1)#1	3.8624(3)	O(3)#1-La(1)-B(1)#4	90.71(16)
B(1)-O(4)	1.350(7)	O(4)#1-La(1)-Te(1)#3	49.21(10)
B(1)-O(5)	1.350(7)	O(4)-La(1)-Te(1)#3	170.43(9)
B(1)-O(1)	1.423(7)	O(5)#2-La(1)-Te(1)#3	108.02(10)
Te(1)-O(2)	1.863(4)	O(2)#3-La(1)-Te(1)#3	26.93(9)
Te(1)-O(3)	1.892(4)	O(2)-La(1)-Te(1)#3	95.15(9)
Te(1)-O(1)	2.052(4)	O(5)#4-La(1)-Te(1)#3	94.50(10)
Te(1)-O(3)#6	2.242(4)	O(1)#4-La(1)-Te(1)#3	94.34(9)
O(4)#1-La(1)-O(4)	139.11(4)	O(3)#1-La(1)-Te(1)#3	124.66(9)
O(4)#1-La(1)-O(5)#2	92.84(13)	B(1)#4-La(1)-Te(1)#3	98.64(13)
O(4)-La(1)-O(5)#2	78.21(14)	O(4)#1-La(1)-La(1)#5	118.77(10)
O(4)#1-La(1)-O(2)#3	72.56(13)	O(4)-La(1)-La(1)#5	38.12(9)
O(4)-La(1)-O(2)#3	147.52(14)	O(5)#2-La(1)-La(1)#5	40.47(10)
O(5)#2-La(1)-O(2)#3	96.47(15)	O(2)#3-La(1)-La(1)#5	131.74(10)
O(4)#1-La(1)-O(2)	141.92(13)	O(2)-La(1)-La(1)#5	83.54(9)
O(4)-La(1)-O(2)	77.81(13)	O(5)#4-La(1)-La(1)#5	111.90(10)
O(5)#2-La(1)-O(2)	85.80(14)	O(1)#4-La(1)-La(1)#5	114.71(10)
O(2)#3-La(1)-O(2)	69.82(16)	O(3)#1-La(1)-La(1)#5	54.52(10)
O(4)#1-La(1)-O(5)#4	77.03(13)	B(1)#4-La(1)-La(1)#5	112.71(13)
O(4)-La(1)-O(5)#4	84.58(13)	Te(1)#3-La(1)-La(1)#5	148.478(16)
O(5)#2-La(1)-O(5)#4	139.90(5)	O(4)#1-La(1)-La(1)#1	38.13(9)
O(2)#3-La(1)-O(5)#4	116.35(14)	O(4)-La(1)-La(1)#1	118.15(10)
O(2)-La(1)-O(5)#4	125.60(14)	O(5)#2-La(1)-La(1)#1	123.99(10)
O(4)#1-La(1)-O(1)#4	117.61(13)	O(2)#3-La(1)-La(1)#1	91.60(9)
O(4)-La(1)-O(1)#4	77.35(13)	O(2)-La(1)-La(1)#1	147.28(10)
O(5)#2-La(1)-O(1)#4	149.50(13)	O(5)#4-La(1)-La(1)#1	39.28(9)
O(2)#3-La(1)-O(1)#4	94.43(14)	O(1)#4-La(1)-La(1)#1	83.95(9)
O(2)-La(1)-O(1)#4	71.44(14)	O(3)#1-La(1)-La(1)#1	72.80(10)
O(5)#4-La(1)-O(1)#4	54.51(12)	B(1)#4-La(1)-La(1)#1	61.69(13)
O(4)#1-La(1)-O(3)#1	75.46(13)	Te(1)#3-La(1)-La(1)#1	64.881(9)

O(4)-La(1)-O(3)#1	64.07(13)	La(1)#5-La(1)-La(1)#1	127.281(18)
O(5)#2-La(1)-O(3)#1	68.53(14)	O(4)-B(1)-O(5)	125.4(5)
O(5)-B(1)-O(1)	115.5(5)	Te(1)#6-O(3)-La(1)#5	113.99(17)
O(2)-Te(1)-O(3)	98.37(19)	B(1)-O(4)-La(1)#5	122.2(4)
O(2)-Te(1)-O(1)	90.84(18)	B(1)-O(4)-La(1)	122.8(4)
O(3)-Te(1)-O(1)	92.07(17)	La(1)#5-O(4)-La(1)	103.75(14)
O(2)-Te(1)-O(3)#6	85.25(19)	B(1)-O(5)-La(1)#8	137.2(4)
O(3)-Te(1)-O(3)#6	75.47(19)	B(1)-O(5)-La(1)#7	95.6(3)
O(1)-Te(1)-O(3)#6	166.21(16)	La(1)#8-O(5)-La(1)#7	100.25(14)
O(2)-Te(1)-La(1)#3	37.64(11)	O(5)#4-La(1)-O(1)#4	54.51(12)
O(3)-Te(1)-La(1)#3	111.76(14)	O(4)-B(1)-O(5)	125.4(5)
O(1)-Te(1)-La(1)#3	123.69(12)	O(4)-B(1)-O(1)	118.8(5)
O(3)#6-Te(1)-La(1)#3	58.09(12)	O(5)-B(1)-O(1)	115.5(5)
La(1)#3-O(2)-La(1)	110.18(16)	O(4)-B(1)-La(1)#7	163.5(5)
Te(1)-O(3)-Te(1)#6	104.53(19)	O(5)-B(1)-La(1)#7	57.8(3)
Te(1)-O(3)-La(1)#5	132.6(2)	O(1)-B(1)-La(1)#7	59.2(3)

Symmetry transformations used to generate equivalent atoms:

#1 -x+1,y+1/2,-z+3/2 #2 x-1/2,y,-z+3/2 #3 -x+1,-y+1,-z+1

#4 -x+3/2,y+1/2,z #5 -x+1,y-1/2,-z+3/2 #6 -x+1,-y,-z+1

#7 -x+3/2,y-1/2,z #8 x+1/2,y,-z+3/2

Table S4. The group structure comparison and optical properties of borotellurites and borotellurates.

	Compounds	Space group	B-O group	Te-O group	Te-B-O group	Δ*n* @1064 nm	Eg (eV)
borotellurites	$Rb_3BaTeB_7O_{15}$	P21/n	$[B_3O_8]$	$[TeO_3]$	$0D[Te^{(iv)}O_3B_{14}O_{28}]$	0.035	4.3
	$LaTeBO_5$	*Pbca*	$[BO_3]$	$[TeO_4]$	$0D[Te^{(iv)}{}_2O_4(BO_3)_2]$	0.08	4.2
borotellurates	$Na_2Y_2TeB_2O_{10}$	$P2_1/c$	$[BO_3]$	$[TeO_6]$	$0D[Te^{(vi)}O_4(BO_3)_2]$	0.04	3.52
	$Na_2Dy_2TeB_2O_{10}$	$P2_1/c$	$[BO_3]$	$[TeO_6]$	$0D[Te^{(vi)}O_4(BO_3)_2]$	n/a	3.53
	$Na_2Ho_2TeB_2O_{10}$	$P2_1/c$	$[BO_3]$	$[TeO_6]$	$0D[Te^{(vi)}O_4(BO_3)_2]$	n/a	3.56
	$Na_2Er_2TeB_2O_{10}$	$P2_1/c$	$[BO_3]$	$[TeO_6]$	$0D[Te^{(vi)}O_4(BO_3)_2]$	n/a	3.59
	$Na_2Tm_2TeB_2O_{10}$	$P2_1/c$	$[BO_3]$	$[TeO_6]$	$0D[Te^{(vi)}O_4(BO_3)_2]$	n/a	3.68
	$Na_2Yb_2TeB_2O_{10}$	$P2_1/c$	$[BO_3]$	$[TeO_6]$	$0D[Te^{(vi)}O_4(BO_3)_2]$	n/a	3.84
	$Na_2Lu_2TeB_2O_{10}$	$P2_1/c$	$[BO_3]$	$[TeO_6]$	$0D[Te^{(vi)}O_4(BO_3)_2]$	n/a	3.9
	$Pb_2Mg_2TeB_2O_{10}$	*Cmca*	$[BO_3]$	$[TeO_6]$	$0D[Te^{(vi)}O_4(BO_3)_2]$	0.077	4.0
	$Ba_2Mg_2TeB_2O_{10}$	*Cmca*	$[BO_3]$	$[TeO_6]$	$0D[Te^{(vi)}O_4(BO_3)_2]$	0.046	4.5
	$Sr_5TeO_2(BO_3)_4$	*P4/mnc*	$[BO_3]$	$[TeO_6]$	$0D[Te^{(vi)}O_2(BO_3)_4]$	0.048	4.28
	$Ba_4B_8TeO_{19}$	*Cc*	$[B_3O_{11}]$	$[TeO_6]$	$3D[B_8Te^{(vi)}O_{19}]$	0.055	3.42

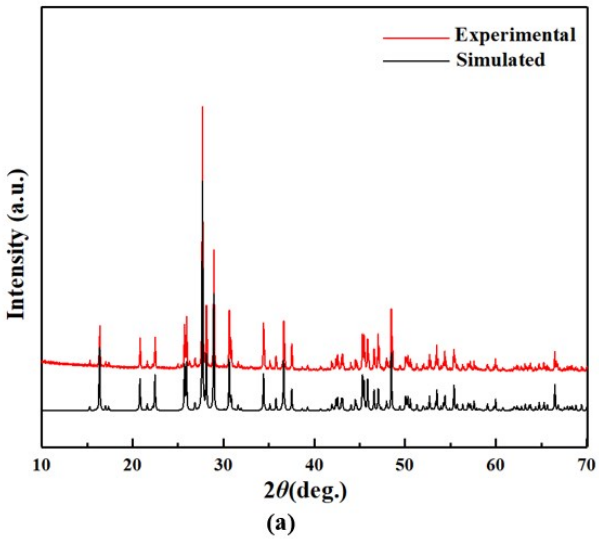

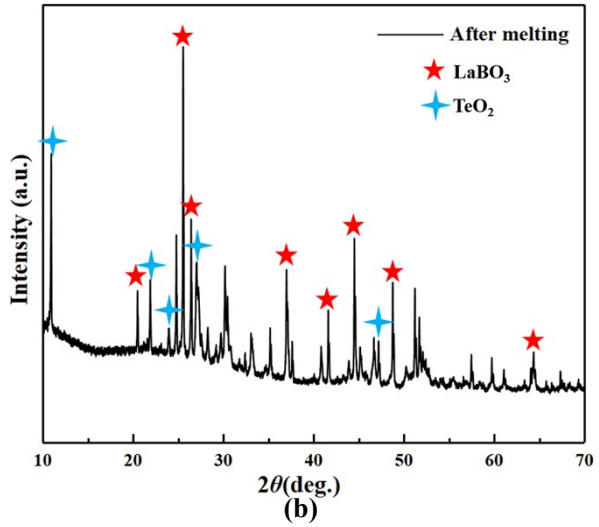

Figure S1. The experimental and calculated XRD diffraction (a) and (b) after melting of $LaTeBO_5$.

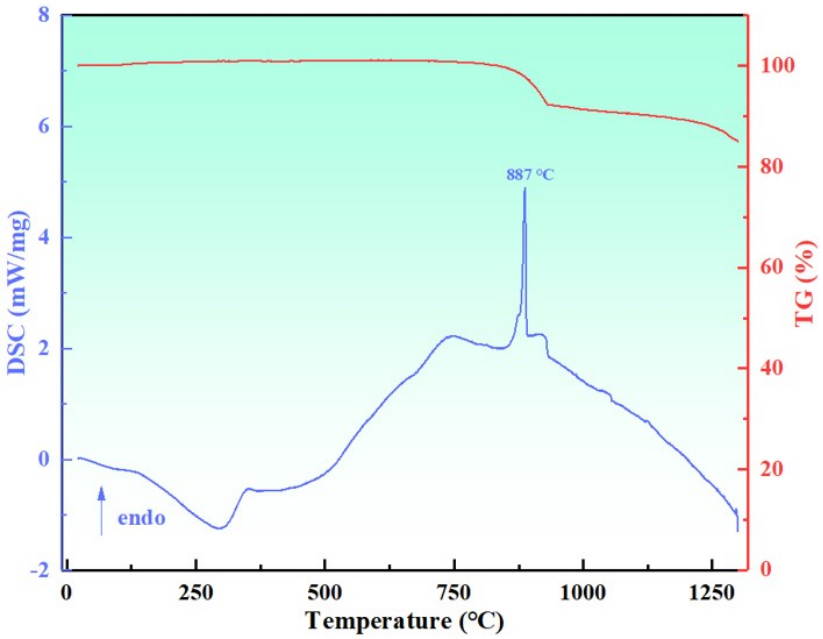

Figure S2. DSC/TG curves of the $LaTeBO_5$

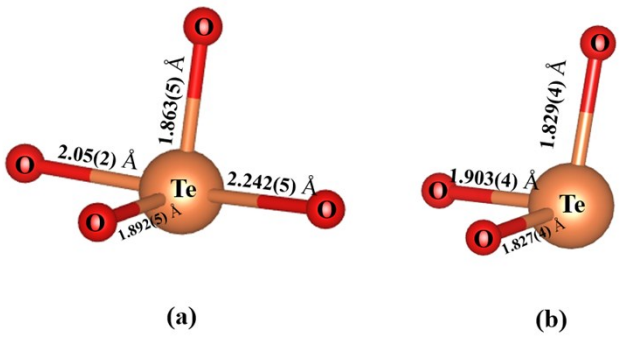

Figure S3. (a) the $[Te^{(iv)}O_4]$ group in $LaTeBO_5$, (b) the $[Te^{(iv)}O_3]$ group in $Rb_3BaTeB_7O_{15}$

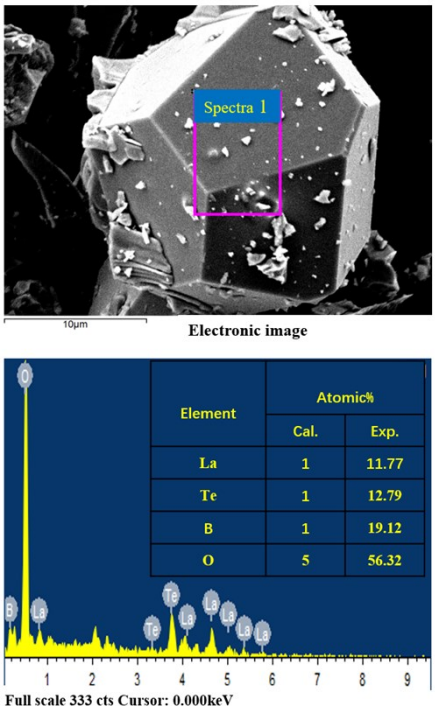

Element	Atomic%	
	Cal.	Exp.
La	1	11.77
Te	1	12.79
B	1	19.12
O	5	56.32

Figure S4. The EDX analysis of $LaTeBO_5$

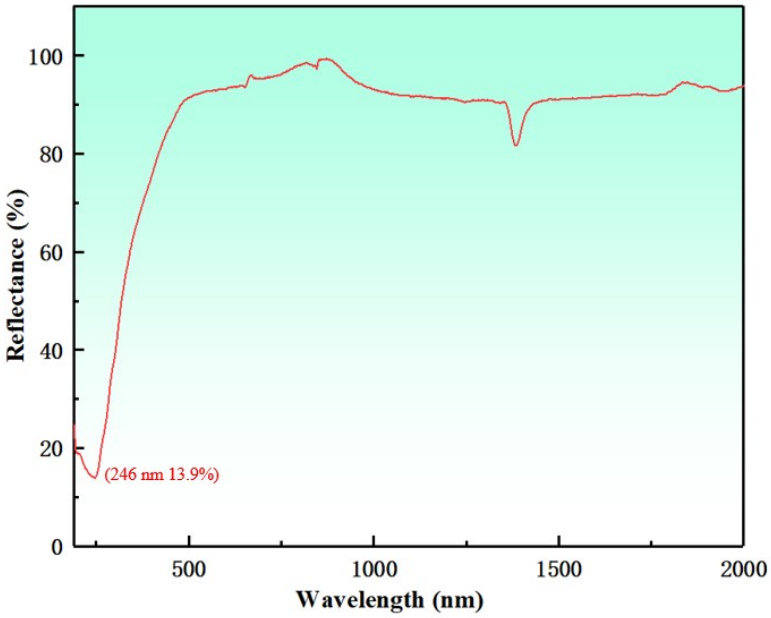

(a)

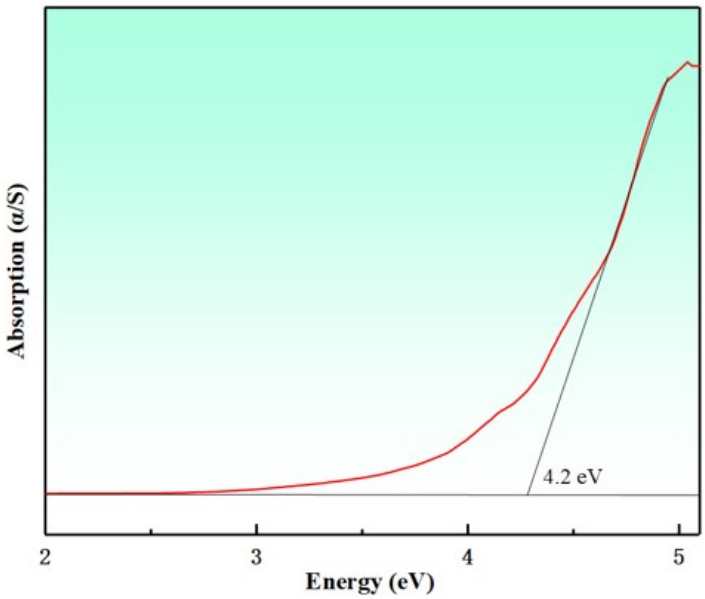

(b)

Figure S5. UV-Vis-IR reflectance spectrum (a) and (b) absorption spectrum of the $LaTeBO_5$.

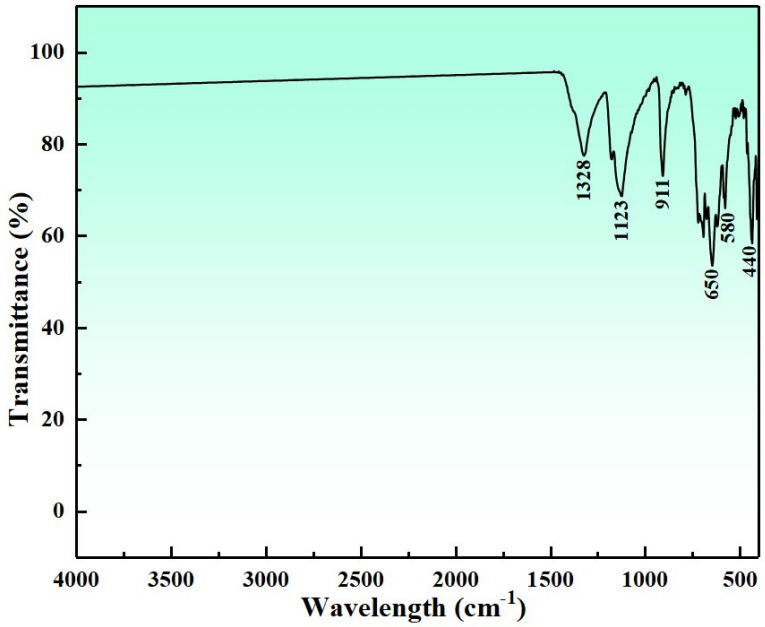

Figure S6. IR spectrum of the $LaTeBO_5$

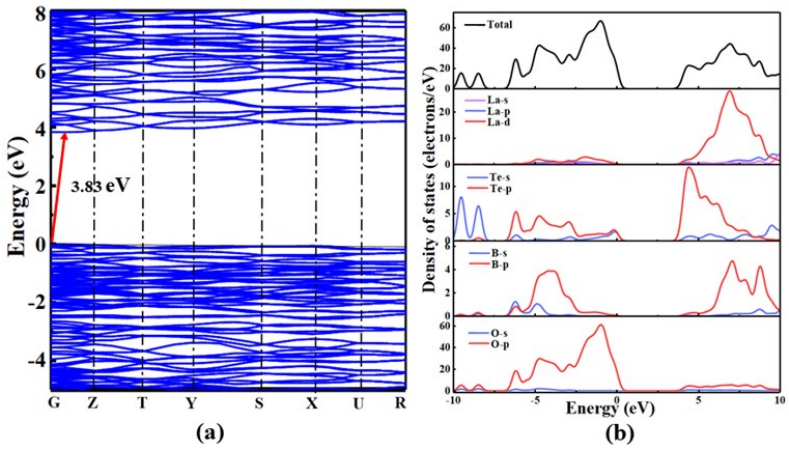

Figure S7. The band structure (a) and (b) total and partial density of states in $LaTeBO_5$.

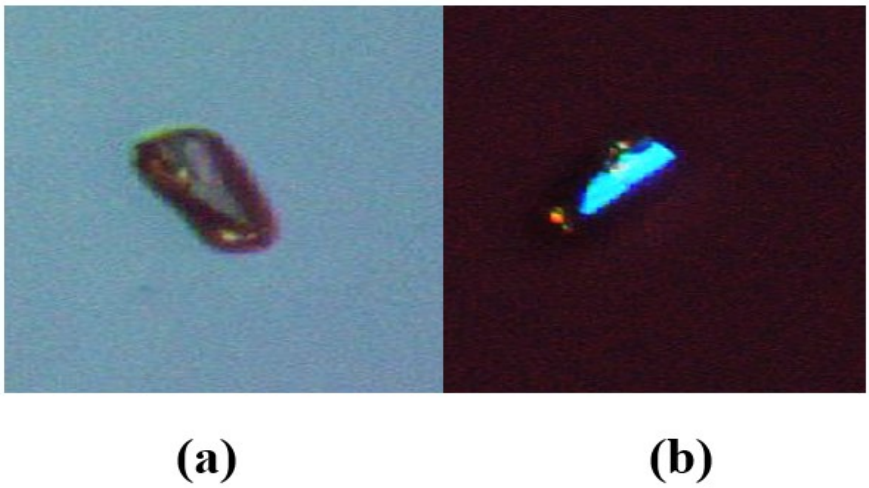

Figure S8. A $LaTeBO_5$ crystal for birefringence measurements by cross-polarized light.

Figure S9. The thickness of $LaTeBO_5$ crystal.

Reference

1. R. Masse, J. Grenier and A. Durif-Varambon, *Bull. Soc. Fr. Mineral. Cristallogr.*, 1967, **90**, 20-23.
2. G. Blasse, *J. Inorg. Nucl. Chem.*, 1968, **30**, 2283-2284.
3. P. Kubelka and F. Munk, *Z. Tech. Phys.*, 1931, **12**, 886-892.
4. S. Clark, M. Segall, C. Pickard, P. Hasnip, M. Probert, K. Refson and M. Payne, *Z. Kristallogr.*, 2005, **220**, 567-570.
5. J. Perdew, J. Chevary, S. Vosko, K. Jackson, M. Pederson, D. Singh, C. Fiolhais and Erratum, *Phys. Rev. B*, 1992, **46**, 6671-6675.
6. J. Perdew, K. Burke and M. Ernzerhof, *Phys. Rev. Lett.*, 1996, **77**, 3865-3868.
7. H. Monkhorst and J. Pack, *Phys. Rev. B*, 1976, **13**, 5188-5192.